The effect of steel and polypropylene fibers on the chloride diffusivity and drying shrinkage of high-strength concrete

Vahid Afroughsabet[a,b,*], Luigi Biolzi[a], Paulo J.M. Monteiro[b]

[a] Department of Architecture, Built Environment and Construction Engineering, Politecnico di Milano, Italy
[b] Department of Civil and Environmental Engineering, University of California, Berkeley, USA

This paper presents an experimental study that investigates the influence of the low fiber content of poly-propylene and hooked-end steel fibers on the properties of high-strength concrete. The study variables include fiber types and fiber contents. The effect of combining both fibers with a total fiber content of 1.0% was also studied in some mixtures. Silica fume, as a supplementary cementitious material, was used at 10% of the cement weight in all fiber-reinforced concrete mixtures. Compressive strength, modulus of elasticity, longitudinal re-sonant frequency, rapid chloride migration and free drying shrinkage tests were performed for different curing ages. The results show that replacement of the cement weight with 10% silica fume improved all of the char-acteristics of the concrete evaluated in this research study. It was observed that the inclusion of fibers, parti-cularly steel fibers, enhanced the mechanical properties of concrete. It was found that the incorporation of polypropylene fibers resulted in a reduction of chloride diffusivity, while introducing steel fibers significantly increased the chloride diffusivity of concrete. Finally, the results showed that hybridization of two types of fibers was an effective way to improve the properties of concrete and specifically reduce the drying shrinkage com-pared with that of the plain concrete.

Keywords: High-strength fiber-reinforced concrete, Fibers, Resonant frequency, Modulus of elasticity, Chloride diffusivity, Free drying shrinkage

1. Introduction

Concrete, with a yearly consumption of more than 25 billion tons [1], is the most used construction material in the world. Currently, the demand for special types of concretes, such as high-performance concrete (HPC) and high-strength concrete (HSC), has also increased throughout the world [2,3]. The addition of a well-defined type of cement, superplasticizer and mineral admixtures has an important influence on the properties of concrete and can lead to a high compressive strength [4,5]. HSCs might be achieved by introducing supplementary cementing materials (SCM), such as silica fume (SF), ground granulated blast-furnace slag (GGBS), fly ash, and natural pozzolans, into the concrete to enhance the stiffness and strength of the interfacial transition zone (ITZ) [6–8]. In general, it is well understood that the substitution of ordinary Portland cement (OPC) with SCMs in concrete reduces the porosity and also converts the pores to smaller sizes compared to conventional concrete. Additionally, the incorporation of SCMs can change the mineralogy of the cement hydrates and subsequently results in a decrease in the motion of chloride ions [9–11].

HSC is more brittle than normal-strength concrete [12] and consequently has a great vulnerability to the initiation and propagation of cracks with different sizes in the body of concrete. Several factors, such as plastic and drying shrinkage, can cause cracks and limit the resistance of concrete against harmful substances [13–15]. It is well documented that fibers in concrete can reduce the brittleness and improve many properties of concrete, including tensile strength, flexural strength, thermal shock strength and toughness [16–22]. Obviously, the inclusion of a given fiber type can be effective only in a limited dimension of crack size, depending on the fiber type, aspect ratio and modulus of elasticity [23]. Hence, hybridization of two or more precisely selected fibers with different sizes and types can create more attractive engineering properties rather than concrete reinforcement with a single type of fiber [24–27]. However, researchers have mainly focused on the progress of hybrid fiber-reinforced concrete (HyFRC) with fiber content greater than 1.0% to produce high-ductility composites. Therefore, there exist very limited experimental data regarding the hybridization of fibers with a volume fraction less than 1.0%, although it can have many applications for civil infrastructure [28,29]. Furthermore, researchers have obtained diverging diffusivity and shrinkage experimental results, which limit a full understanding of these features [30–32].

For instance, Kaïkea et al. [33] showed that introducing 2%

Received 23 January 2017;
Received in revised form 27 November 2017;
Accepted 28 November 2017
Available online 02 December 2017

* Corresponding author. Department of Architecture, Built Environment and Construction Engineering, Politecnico di Milano, Italy.
E-mail addresses: vahid.afroughsabet@polimi.it (V. Afroughsabet), luigi.biolzi@polimi.it (L. Biolzi), monteiro@ce.berkeley.edu (P.J.M. Monteiro).

corrugated steel fibers in concrete resulted in a reduction up to 24% on the shrinkage of HPC. In another study, Choi et al. [34] reported that the drying shrinkage of specimens reinforced with 0.1% nylon and 0.1% steel fibers was reduced more than two times compared to that of the plain concrete. Moreover, a reduction up to 65% on the shrinkage strain of fiber-reinforced concrete (FRC) was recorded [35]. On the other hand, other researchers indicated that fibers had negligible influence on the shrinkage of concrete [36–38]. Similarly, there is no clear consensus on the effect of fibers on the diffusivity of concrete. Behfarnia and Behravan [39] showed that the chloride penetration depth of concretes reinforced with steel fibers reduced by 15%, while a slight increase in the chloride penetration depth of steel FRC was reported by Frazão et al. [40]. The results obtained by Toutanji et al. [32] indicated that the inclusion of polypropylene fibers resulted in a reduction in the chloride penetration resistance of concrete. Conversely, research by Ramezanianpour et al. [31] showed that concrete samples made with polypropylene fibers had higher resistance against the chloride penetration. Crack width is an important factor controlling the corrosion of steel reinforcing bars; therefore, it is recommended to limit the crack width on the tensile surface of reinforced concrete to 330 μm [41]. However, the maximum allowable crack width based on the requirement of ACI 224 [42] is 100 μm. Blunt et al. [43] indicated that HyFRC due to their higher resistance to cracking can effectively postpone the rebar corrosion and reduce the corrosion rate.

The objective of this study is to investigate the properties of HSC manufactured with polypropylene and steel fibers individually and in combination, with fiber volume fraction lower than 1.0%. Compressive strength, modulus of elasticity, longitudinal resonant frequency, rapid chloride migration and the drying shrinkage test were measured for different curing ages. The longitudinal resonant frequency was used as a non-destructive technique to measure dynamic and static modulus of elasticity of concrete. The findings of this research can contribute to promoting the application of HSC were manufactured with steel and polypropylene fibers in different concrete structures.

2. Materials and methods

To assess the effect of fibers on the mechanical and durability features of HSC, twelve different concrete mix proportions were analyzed. The experimental matrix included concrete without fibers, concrete containing polypropylene fibers, concrete containing steel fibers and HyFRC. A schematic diagram of the experimental program is shown in Fig. 1. All the tests were carried out for 7, 28, and 91 days to study the effect of curing time on the results, except the free drying shrinkage tests, which were conducted for the specimens cured for 28 days.

2.1. Materials

The binder materials used in this study were ASTM Type 1 Portland cement and silica fume with specific surface of 300 and 14000 m^2/kg, respectively. Their chemical compositions and physical properties are given in Table 1. Both natural sand, with a 3.4 fineness modulus, and crushed gravel, with a nominal maximum size of 19 mm, were used as the aggregates at a volume fraction of 50%. The water absorption, specific gravity and other relevant data for the aggregates are given in Table 2, and their grading curves are shown in Fig. 2. To achieve the desired workability in different concretes, a Carboxylic 110 M, produced by the BASF factory, was used as a superplasticizer (SP). Hooked-end steel fibers and polypropylene (PP) fibers with length and aspect ratios of 60 mm and 80 and 12 mm and 545 were used in this study, respectively. The properties and the pictures of fibers are given in Table 3.

2.2. Concrete mixtures and mixing procedure

The water-binder ratio was maintained at 0.3 for all mixtures. Silica Fume (SF) was added as a cement replacement for 10% of the mass to FRCs. Additionally, a mix containing SF and without fibers was manufactured to study its influence on the results. A pan mixer was used for the preparation of all the mixes. Prior to adding the raw materials, the surface of the pan mixer was cleaned with a wet towel to avoid the absorption of aggregates moisture by the mixer. To fabricate uniform high-strength fiber-reinforced concrete (HSFRC), several mixing procedures have been tried and the following one was chosen. Initially, the fine aggregate, cement and SF (if applicable) were mixed for one min. Afterward, approximately half of the water including SP, was introduced into the mixer; the ingredients were further mixed for two min. The Saturated Surface Dry (SSD) coarse aggregates and remaining mixing water were then introduced, and the mixing was carried on for another 5 min. In the last step, fibers were added gradually to the rotating mixer and were mixed for an additional 5 min to obtain a homogenous mixture. Details of mix proportions and the results of a slump test and density of hardened concretes are summarized in Table 4. The content of SP in that table is given as a percentage of the total mass of the binder. To determine the workability of fresh concrete, slump tests were performed as per ASTM C143 [44] during the preparation of the concrete mixes. The specimens were molded with different dimensions that matched the requirements of their standards test. The samples were covered with a wet plastic sheet to prevent them from dripping water in the first 24 h of curing. Then, the concrete specimens were demolded and immersed in lime-saturated water at 23 °C until reaching their testing ages. For each test, three samples were prepared, and the average value was demonstrated as the final result.

2.3. Testing methods

2.3.1. Mechanical tests

Compression and static modulus of elasticity tests were conducted on the cylindrical specimens, with dimensions of 100 × 200 mm, using a 3000-kN universal compression machine in accordance with ASTM C39 [45] and ASTM C469 [46], respectively. To monitor the strain of specimens subjected to loading, two strain gauges were attached vertically at the middle height and opposite surfaces of each sample, and deformations were measured by using a 30 channel data logger.

2.3.2. Longitudinal resonant frequency test

The longitudinal resonant frequencies of the 100 × 100 × 400 mm beams were determined according to BS 1881-209 [47]. An adaptable grease was applied to the surfaces of the concrete prisms to decrease the air pockets between the interfaces of concrete specimens and transducers. The value of the frequency resulting in the maximum amplitude at the pick-up point is counted as the longitudinal resonant frequency of the specimen. Additionally, by applying the longitudinal resonant frequency test results in Eq. (1) it is possible to calculate the dynamic modulus of elasticity $E_{d,r}$ of concrete specimens in GPa.

$$E_{d,r} = 4n^2l^2\rho 10^{-15} \quad (1)$$

where l is the length of the sample (mm), n is the longitudinal resonant frequency (Hz) and ρ is the density of hardened concrete (kg/m^3). The subscript r means that the resonant frequency testing technique was used to calculate the dynamic modulus of elasticity.

There are different empirical correlations that have been developed to drive the static modulus of elasticity from the results of the dynamic modulus of concrete. Eq. (2) indicates one generally accepted correlation in UK practice for conventional concrete [48] that the static modulus of elasticity E_{cm} in GPa can be calculated by using the results of dynamic modulus of elasticity $E_{d,r}$:

$$E_{cm} = 1.25E_{d,r} - 19 \quad (2)$$

Eqs. (1) and (2) were developed for normal strength concrete with compressive strengths ranging from 30 to 60 MPa. Nevertheless, in the present study, their potential implementation for HSFRC has been

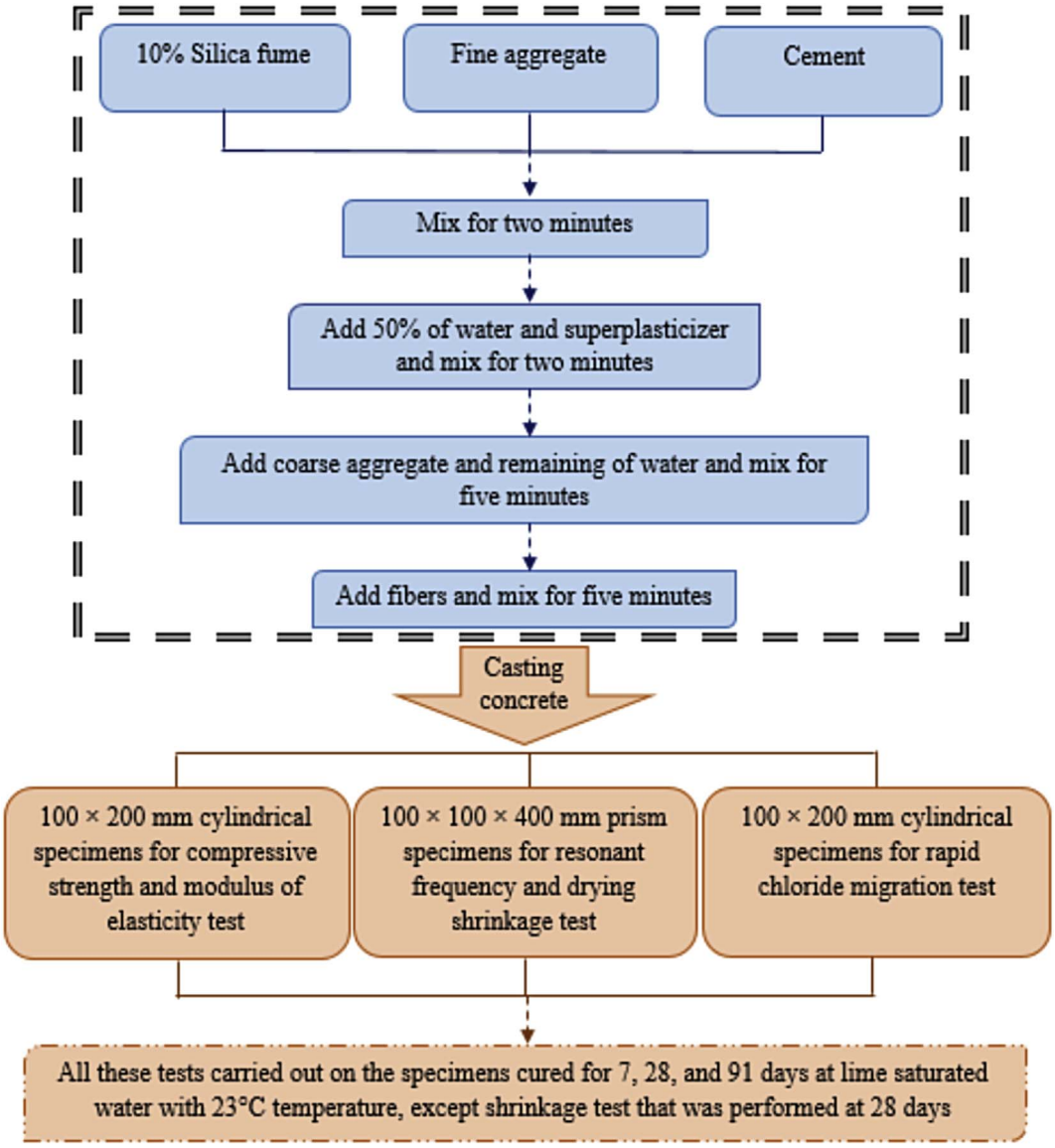

Fig. 1. Scheme of the study procedure.

Table 1
Chemical composition and physical properties of cementitious materials.

Item	Cementitious materials (%)	
	Cement	Silica fume
SiO_2	21.2	93.0
Al_2O_3	5.4	1.7
Fe_2O_3	3.4	1.2
MgO	1.4	1.0
Na_2O	–	0.6
K_2O	–	1.1
CaO	63.9	0.3
	Compounds	
C_3S	51.5	–
C_2S	22.0	–
C_3A	6.4	–
C_4AF	10.5	–
	Physical properties	
Specific gravity (kg/m^3)	3150	2210
Specific surface (m^2/kg)	300	14,000

Table 2
Physical properties of the aggregates.

Aggregate type	Maximum size aggregate (mm)	Water absorption (%)	Specific gravity	Fineness modulus
Fine aggregate	4.75	1.92	2.61	3.4
Coarse aggregate	19.0	0.56	2.69	–

investigated.

2.3.3. *Free drying shrinkage test*

The free drying shrinkage test was performed on prismatic samples as per ASTM C 157 [49]. Upon removal of specimens from the molds, pins were attached to the surfaces of the specimens. The samples were kept in lime-saturated water for 30 min to minimize variation in length due to variation in temperature. After that, the specimens were removed from the water storage and wiped with a damp cloth; then, the initial comparator reading was measured immediately. Then, the specimens were stored in lime-saturated water at 23 °C until they reached the age of 28 days. The drying shrinkage test was performed on the air-

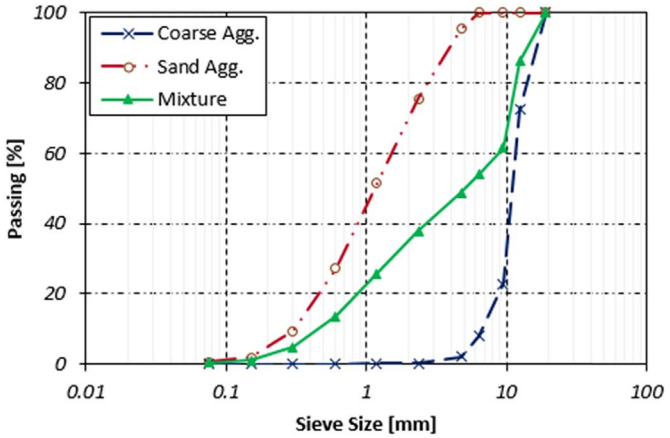

Fig. 2. Grading curves of aggregates.

stored specimens in a room with temperature of 23 °C and 50% relative humidity; consecutive readings were carried out after curing for 4, 7, 14, and 28 days and after 8, 16, 32, and 64 weeks. The length variation was measured, whereby a dial gage extensometer with 300-mm gage length and a reading resolution of 0.002 mm was used.

2.3.4. Rapid chloride migration test

The non-steady-state chloride migration coefficient [50] was used to measure the resistance of concrete samples against chloride penetration. This test was performed on the 50 mm-high specimens that were obtained from the 100-mm cylindrical specimens. The samples were fit with rubber sleeves and secured with two clamps to prohibit the leakage of anolyte solution (0.3 M sodium hydroxide (NaOH)), from the interfaces between specimens and sleeves, to the catholyte solution (10% sodium chloride (NaCl)). Thereafter, the specimens inside the sleeves were exposed to anolyte solution and placed on a plastic support in a catholyte reservoir. An initial external electrical potential of 30 V was applied, and the initial current was recorded. Based on the value of the current, the next voltage and test duration were determined; consequently, the new electrical potential was applied to the specimen to force the chloride ions to migrate from the NaCl solution into the specimen. Finally, the specimen was axially split across its circular cross section. The split surfaces were sprayed with 0.1 M silver nitrate ($AgNO_3$) solution, and the penetration of silver chloride precipitates was measured. Finally, the chloride migration coefficient was calculated for this penetration depth using the following equation:

$$D_{nssm} = \frac{0.0239(273 + T)L}{(U - 2)t}\left(x_d - 0.0238\sqrt{\frac{(273 + T)Lx_d}{(U - 2)}}\right) \quad (3)$$

where D_{nssm} is the non-steady-state migration coefficient ($\times 10^{-12}$ m^2/s); U is the absolute value of the applied voltage (V); T is the average initial and final temperature in the anolyte solution (°C); L is the thickness of the specimen (mm); x_d is the average value of the penetration depths (mm); and t is the duration of the test (h).

3. Results and discussions

3.1. Workability

The effects of inclusion fibers and the addition of SF on the slump test results are shown in Table 4. The inclusion of SF in the plain concrete by using an equal dosage of SP led to a reduction in the slump value. Furthermore, concretes manufactured with PP fibers showed lower slump values; thus, a higher content of SP was added to maintain the same workability. The results indicate that an increase in the volume fraction of PP fibers caused a greater reduction in the workability of concrete. The incorporation of steel fibers also has a negative influence on the properties of fresh concrete. The long steel fibers and aggregates interlock in the body of concrete and lead to a reduction in the slump value. However, the presence of SF in FRC increased the cohesiveness of mixes and led to a better distribution of fibers in the concrete [51]. The results also showed that the replacement of a portion of steel fiber with PP fiber in HyFRC caused a reduction in the slump test results. Among the different mixes studied in this work, the lowest slump value was attained by the mix comprising 0.55% steel and 0.45% PP fibers.

3.2. Compressive strength

The compressive strength test results for different FRCs containing different fiber contents and types are presented in Table 5 and shown in Fig. 3. The replacement of cement mass with 10% SF resulted in an increase in the compressive strength. For instance, the compressive strength of this mix was increased by 7%, 9%, and 11% for curing ages of 7, 28, and 91 days, respectively, compared to those of the plain concrete. This can be attributed to the formation of an additional C-S-H gel significantly at later ages, which is the main strength contributing compound. Moreover, SF also fills in the capillary pores and improves the features of the ITZ and microstructure of the cement matrix [52,53].

The addition of fibers in concrete also led to an increase in the compressive strength. Higher strength is achieved in mixes containing higher fiber volume fraction. The increase in the strength of polypropylene fiber-reinforced concretes ranged from 8% to 17%, while for steel fiber-reinforced concretes, varied from 11% to 25%, depending on the fiber volume fraction and testing age. As shown in Table 5, the effectiveness of the steel fibers is higher than that of the PP fibers regarding the enhancement of the compressive strength. The reason for that is the higher strength, length, and modulus of elasticity of steel fibers, compared to those of PP fibers, which subsequently increase the effectiveness of steel fibers in bridging macro-cracks and result in an enhanced strength [54]. The results of HyFRC indicate that the combined use of steel and PP fibers can considerably increase the compressive strength over that of the mix without fibers. In general, the increase in compressive strength of these mixes ranged from 18% to

Table 3
Properties of hooked-end steel and PP fibers.

Type of fiber	Length l (mm)	Diameter d (mm)	Aspect ratio l/d	Density (g/cm^3)	Tensile strength (N/mm^2)	Picture of fibers
Hooked-end steel (ST)	60	0.75	80	7.8	1050	
Polypropylene (PP)	12	0.022	545	0.91	350	

Table 4
Mix proportions of concrete mixes.

Mix No.	Mixture ID	W/B	Water	Cement	Silica Fume	Fine Agg.	Coarse Agg.	Fiber volume fraction (%)		SP (%)[a]	Slump (mm)	Density (kg/m^3)
			(kg/m^3)					ST	PP			
1	Plain	0.3	156	520	–	860	886	–	–	1.0	170	2437
2	SF10	0.3	156	468	52	851	877	–	–	1.0	145	2416
3	PP0.15	0.3	156	468	52	849	875	–	0.15	1.2	130	2413
4	PP0.30	0.3	156	468	52	847	873	–	0.30	1.3	115	2408
5	PP0.45	0.3	156	468	52	845	871	–	0.45	1.4	80	2401
6	ST0.25	0.3	156	468	52	847	873	0.25	–	1.1	150	2433
7	ST0.50	0.3	156	468	52	844	870	0.50	–	1.1	120	2449
8	ST0.75	0.3	156	468	52	841	867	0.75	–	1.2	125	2464
9	ST1.0	0.3	156	468	52	838	863	1.00	–	1.2	80	2478
10	PP0.15ST0.85	0.3	156	468	52	838	863	0.85	0.15	1.2	85	2462
11	PP0.30ST0.70	0.3	156	468	52	838	863	0.70	0.30	1.2	95	2457
12	PP0.45ST0.55	0.3	156	468	52	838	863	0.55	0.45	1.2	50	2454

[a] Percentage of total weight of cementitious material.

27% compared with that of the plain concrete, depending on the fiber hybridization and testing age. An increase in the content of PP fibers in HyFRC led to a reduction in the compressive strength of concrete. This can be related to an increase in the porosity of mixes that were manufactured with higher amounts of PP fibers due to the poor dispersion of fibers [55].

The effect of specimen shape on the results of the compression tests for different concrete specimens is shown in Table 5. In this research, compression tests were carried out on the cylindrical specimens. However, the results of cubic specimens that already published by Afroughsabet and Ozbakkaloglu [14] have been provided to investigate the effect of specimen shape on strength. As expected, the cylindrical specimens obtained lower strength compared to the cubic specimens. This result is an agreement with the findings of other researchers [56]. The average ratio for concretes without fibers is equal to 0.88 for different curing ages. This ratio for concrete containing PP and steel fibers ranged from 0.88 to 0.90 and 0.90 to 0.93, respectively, depending on the age of the test. It was also observed that the difference between cylindrical and cubic strength has been reduced by the hybridization of fibers; the ratio varied from 0.90 to 0.94.

3.3. Longitudinal resonant frequency

This method allows us to investigate the uniformity and relative quality of concrete to demonstrate the existence of voids and degree of cracking. Generally, an increase in the crack size or porosity of specimens results in a reduction in the resonant frequency [57]. On the other hand, with an increase in the density of concrete specimens, a higher resonant frequency will be achieved. The variations of the longitudinal resonant frequency of different concrete specimens are shown in Fig. 4 and Table 6. The results indicate that introducing of SF in concrete slightly increased the resonant frequency of the control specimen, and a maximum frequency of 5550 Hz was recorded after 91 days. This can be due to the increased bond between the aggregates and cement matrix and improved properties of the cement paste. As shown in Fig. 4, as curing time increased, the resonant frequency of all specimens increased significantly. The reason for that was the hydration process of cementitious materials, which in turn improved the microstructure of concrete, and led to a higher frequency.

The results showed that the addition of PP fibers resulted in a reduction in the resonant frequency, while introducing steel fibers led to an increase in the frequency of specimens. Additionally, an increase in the PP fiber content caused a greater reduction in the resonant frequency compared to that of plain concrete. For instance, the 28-day longitudinal resonant frequencies of the mixes fabricated with 0.15%, 0.3%, and 0.45% PP fibers were 5212, 5187, and 5169 Hz, respectively, whereas plain concrete had a frequency of 5215 Hz. As shown in Table 4, an increase in the content of PP fibers resulted in a reduction in the workability of concrete that consequently may cause higher porosity in those mixes. Therefore, the reduction in the resonant frequency of polypropylene fiber-reinforced concretes may be attributed to an increase in porosity of concrete as a result of the inclusion of PP fibers.

Table 5
Compressive strength of fiber-reinforced concrete test results.

Mix No.	Mixture ID	Compressive strength of cylindrical 100 mm specimen (MPa)			Compressive strength of cubic 100 mm specimen (MPa)[a]			Ratio of cylindrical to cubic specimens strength		
		7 Days	28 Days	91 Days	7 Days	28 Days	91 Days	7 Days	28 Days	91 Days
1	Plain	61.9	71.8	77.5	71.2	82.6	88.3	0.87	0.87	0.88
2	SF10	66.4	78.5	86.2	75.2	88.8	98.0	0.88	0.88	0.88
3	PP0.15	66.8	80.1	87.4	74.9	91.2	98.6	0.90	0.88	0.89
4	PP0.30	68.5	80.6	87.1	75.7	91.5	101.4	0.90	0.88	0.86
5	PP0.45	68.1	83.3	90.9	77.1	92.8	100.3	0.88	0.90	0.90
6	ST0.25	68.8	82.7	91.7	76.1	92.3	98.5	0.93	0.90	0.93
7	ST0.50	71.5	84.6	93.5	77.4	93.8	102.0	0.92	0.90	0.92
8	ST0.75	73.2	85.2	94.4	78.3	95.0	102.6	0.93	0.90	0.92
9	ST1.0	74.8	87.8	96.7	79.9	98.7	104.3	0.94	0.89	0.93
10	PP0.15ST0.85	75.4	89.3	98.1	80.1	97.5	104.0	0.94	0.92	0.94
11	PP0.30ST0.70	74.3	87.4	97.0	81.4	96.6	103.2	0.91	0.92	0.94
12	PP0.45ST0.55	72.9	87.1	95.3	77.9	95.3	102.8	0.94	0.90	0.93

[a] These results were included in another paper by the author [14].

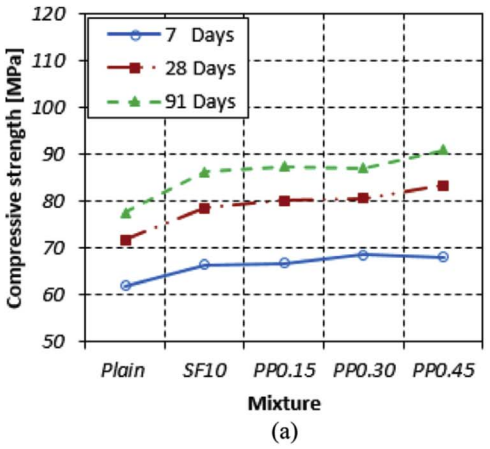

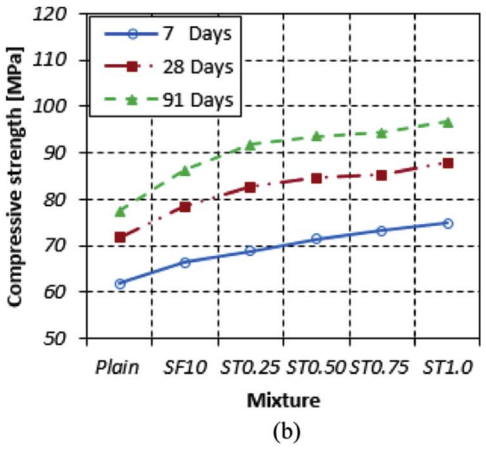

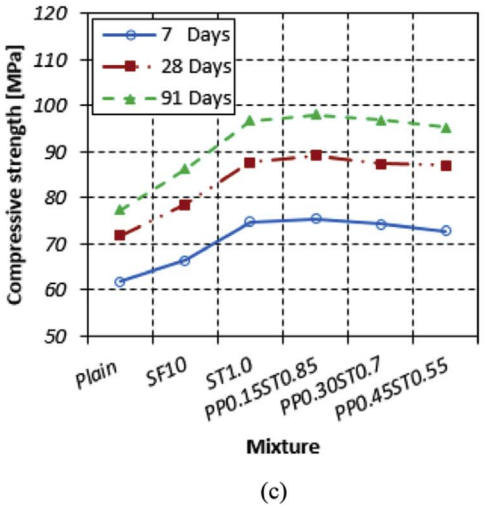

Fig. 3. Compressive strengths of different fiber-reinforced concretes: (a) polypropylene fiber-reinforced specimens, (b) steel fiber-reinforced specimens, and (c) hybrid fiber-reinforced specimens.

The resonant frequency of steel fiber-reinforced concretes ranged from 5028-5057, 5273-5318, and 5562-5604 Hz after 7, 28, and 91 days, respectively, depending on the fiber content. Among different steel fiber volume fractions considered in this study, the maximum frequency was achieved by using 1.0% steel fibers to the concrete. This improvement can be attributed to the increased density of hardened specimens due to the higher density of steel fiber than polymer like PP fiber. Furthermore, the results of HyFRC show that replacement of a fraction of steel with PP fibers resulted in a decrease in the resonant frequency of the specimens. However, all of these specimens had higher frequency with respect to that of the reference specimen.

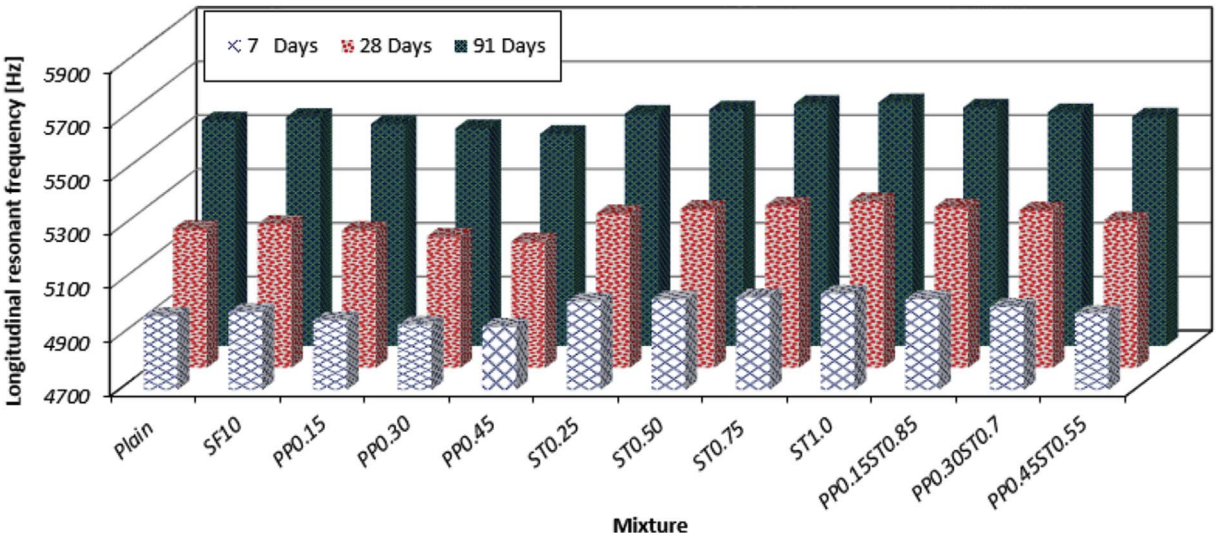

Fig. 4. Longitudinal resonant frequency of different fiber-reinforced concretes.

Table 6
Results of longitudinal resonant frequency and dynamic modulus of elasticity tests.

Mix No.	Mixture ID	Longitudinal resonant frequency (Hz)			Dynamic modulus of elasticity[a], $E_{d,r}$ (GPa)		
		7 Days	28 Days	91 Days	7 Days	28 Days	91 Days
1	Plain	4974	5215	5537	38.59	42.42	47.82
2	SF10	4988	5234	5550	38.47	42.36	47.63
3	PP0.15	4957	5212	5524	37.95	41.95	47.12
4	PP0.30	4941	5187	5508	37.62	41.46	46.75
5	PP0.45	4934	5169	5487	37.41	41.06	46.26
6	ST0.25	5028	5273	5562	39.37	43.29	48.17
7	ST0.50	5035	5290	5577	39.73	43.86	48.75
8	ST0.75	5044	5302	5598	40.12	44.33	49.42
9	ST1.0	5057	5318	5604	40.56	44.85	49.81
10	PP0.15ST0.85	5036	5296	5585	39.96	44.19	49.15
11	PP0.30ST0.70	5007	5284	5568	39.42	43.90	48.75
12	PP0.45ST0.55	4982	5247	5551	38.98	43.24	48.39

[a] Dynamic modulus of elasticity of the specimens calculated using Eq. (1).

3.4. Dynamic modulus of elasticity

The dynamic modulus of elasticity of different specimens has been calculated by using the longitudinal resonant frequency test results as presented in Table 6. Because the density of specimens has an influence on the results, it was observed that concrete containing SF had a slightly lower dynamic modulus of elasticity due to the lower density compared to that of the plain concrete. Furthermore, the results show that the addition of PP fibers led to a reduction in the dynamic modulus of elasticity. The inclusion of 0.45% PP fiber caused a reduction of up to 3% in the dynamic modulus of elasticity after 28 days over that of the plain concrete. This can be explained by the increased porosity of concrete through the inclusion of PP fibers [58,59]. The dynamic modulus of elasticity for steel fiber-reinforced concretes ranged from 39.37 to 49.81 GPa, depending on the fiber volume fraction and testing age. In general, there is an increase in the dynamic elasticity of concrete as the steel fibers content increases. This can be attributed to the higher elastic modulus of steel fibers and increased density of specimens, which consequently improved the dynamic properties of concrete. The presence of SF, as a cement replacement, also promoted the dispersion of steel fibers in concrete and caused an enhancement in the results. The results showed that the combination of two types of fibers led to a negligible decrease in the results when compared to the mix containing 1.0% steel fiber.

3.5. Static modulus of elasticity

There is a direct correlation between density and modulus of elasticity in homogeneous materials. However, in heterogeneous, multiphase materials, such as concrete, density, modulus of elasticity of the principal constituents, and the characteristics of the transition zone determine the elastic modulus behavior of the composite [60,61]. The static modulus of elasticity of different FRCs are shown in Fig. 5 and summarized in Table 7. The results of the present study demonstrate that the addition of SF caused an increase of up to 4% in the elastic modulus of concrete. The improvement in elasticity can be due to the densification of the ITZ between paste and aggregate, in addition to the increased density of the concrete caused by the fineness of the SF.

The introduction of fibers of any type and content led to an increase in the static modulus of the concrete when compared to that of the plain concrete. As shown in Fig. 5, a maximum increase of up to 6% was attained through the addition of 0.45% PP fiber. Furthermore, the increase in the static modulus of the elasticity of steel fiber-reinforced concretes ranged from 3% to 12%, depending on the fiber volume fraction and curing time. The efficiency of steel fibers was higher than that of PP fibers due to their higher strength and modulus of elasticity, which subsequently improved the static modulus of the concrete. As shown in Table 7, among different mixes considered in this study, the highest elastic modulus was attained by the mix containing 0.3% PP and 0.7% steel fibers, which gained a 91-day elastic modulus of 41.9 GPa. Aslani and Nejadi [62] also reported that higher modulus of elasticity was achieved by hybridization of PP and steel fibers compared to monotype use of fibers.

The results of secant modulus of elasticity *Ecm,* calculated based on the results of dynamic modulus of elasticity, and the ratio of *Ecm* to the experimental test results are also presented in Table 7. The ratio of *Ecm* to the experimental test results ranged from 0.83 to 1.06, depending on the testing age and type of reinforcement. This result shows a good agreement with the finding of Hassan and Jones [63], who found errors in the range of 0.9–0.98. As shown in the table, the secant modulus of elasticity obtained from the empirical correlation was underestimated at 7 and 28 days, while the results after 91 days were slightly overestimated. The results also indicate that the trend of the static modulus of elasticity and those determined from the empirical relationship are different for concrete containing PP fibers. Based on Eqs. (1) and (2), there is a direct relationship between the density and resonant frequency of concrete and its secant modulus of elasticity. Therefore, values were reduced due to a reduction in the density and longitudinal resonant frequency of concretes reinforced with PP fibers. Because the inclusion of steel fibers increased the aforementioned features of concrete, there is a similar behavior between the results of concrete manufactured with steel fibers.

3.6. Rapid chloride migration coefficient

Permeability is considered to be the most important feature for the long-term performance of a reinforced concrete structure [64–66]. Microstructural properties like the size, distribution, and interconnection of micro-cracks and pores are the main factors that affecting the permeability of concrete [18,67]. The calculated chloride migration coefficients of different concretes with and without fibers are shown in Fig. 6 and presented in Table 8. Based on the chloride migration coefficient of specimens and criteria provided in Table 9 [68], the resistance to chloride penetration of different concretes was classified and summarized in Table 8. The addition of SF significantly reduced the chloride migration coefficient of concrete. Substituting 10% of cement weight with SF led to a reduction of up to 54%, 76%, and 78% at 7, 28, and 91 days, respectively, when compared to those of the reference concrete. This may have contributed to the effect of SF on the formation of a secondary C-S-H gel, refined the pore size, and produced an enhanced transition zone that consequently caused a reduction in the chloride migration coefficient of concrete. Toutanji et al. [32] indicated

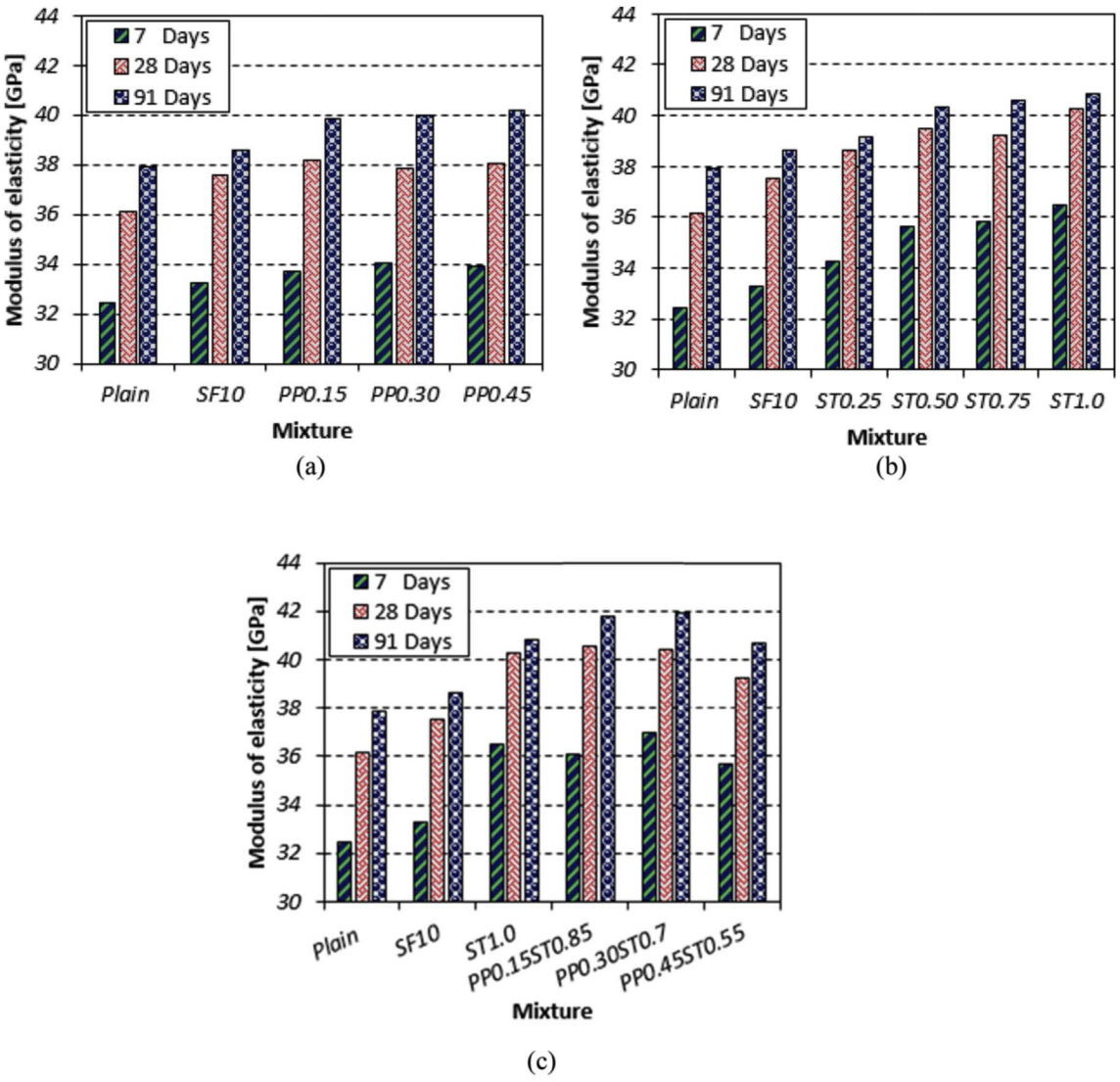

Fig. 5. Static modulus of elasticity of different fiber-reinforced concretes: (a) polypropylene fiber-reinforced specimens, (b) steel fiber-reinforced specimens, and (c) hybrid fiber-reinforced specimens.

Table 7
Modulus of elasticity of fiber-reinforced concrete test results.

Mix No.	Mixture ID	Static modulus of elasticity[a] (GPa)			Modulus of elasticity[b], *Ecm* (GPa)			Average ratio of *Ecm* to static modulus of elasticity		
		7 Days	28 Days	91 Days	7 Days	28 Days	91 Days	7 Days	28 Days	91 Days
1	Plain	32.45	36.14	37.89	29.23	34.02	40.77	0.89	0.92	1.06
2	SF10	33.27	37.56	38.61	29.09	33.95	40.54			
3	PP0.15	33.68	38.19	39.82	28.43	33.44	39.91	0.83	0.86	0.98
4	PP0.30	34.05	37.84	39.95	28.03	32.83	39.44			
5	PP0.45	33.92	38.03	40.21	27.76	32.32	38.83			
6	ST0.25	34.29	38.67	39.13	30.21	35.12	41.21	0.87	0.92	1.05
7	ST0.50	35.61	39.46	40.34	30.67	35.83	41.94			
8	ST0.75	35.83	39.22	40.57	31.15	36.41	42.77			
9	ST1.0	36.48	40.30	40.84	31.70	37.06	43.26			
10	PP0.15ST0.85	36.09	40.57	41.76	30.95	36.24	42.44	0.84	0.89	1.01
11	PP0.30ST0.70	36.95	40.42	41.90	30.28	35.88	41.94			
12	PP0.45ST0.55	35.70	39.26	40.66	29.73	35.05	41.49			

[a] Static modulus of elasticity of the test specimens calculated in accordance with ASTM C469.
[b] Modulus of elasticity of the specimens calculated using Eq. (2).

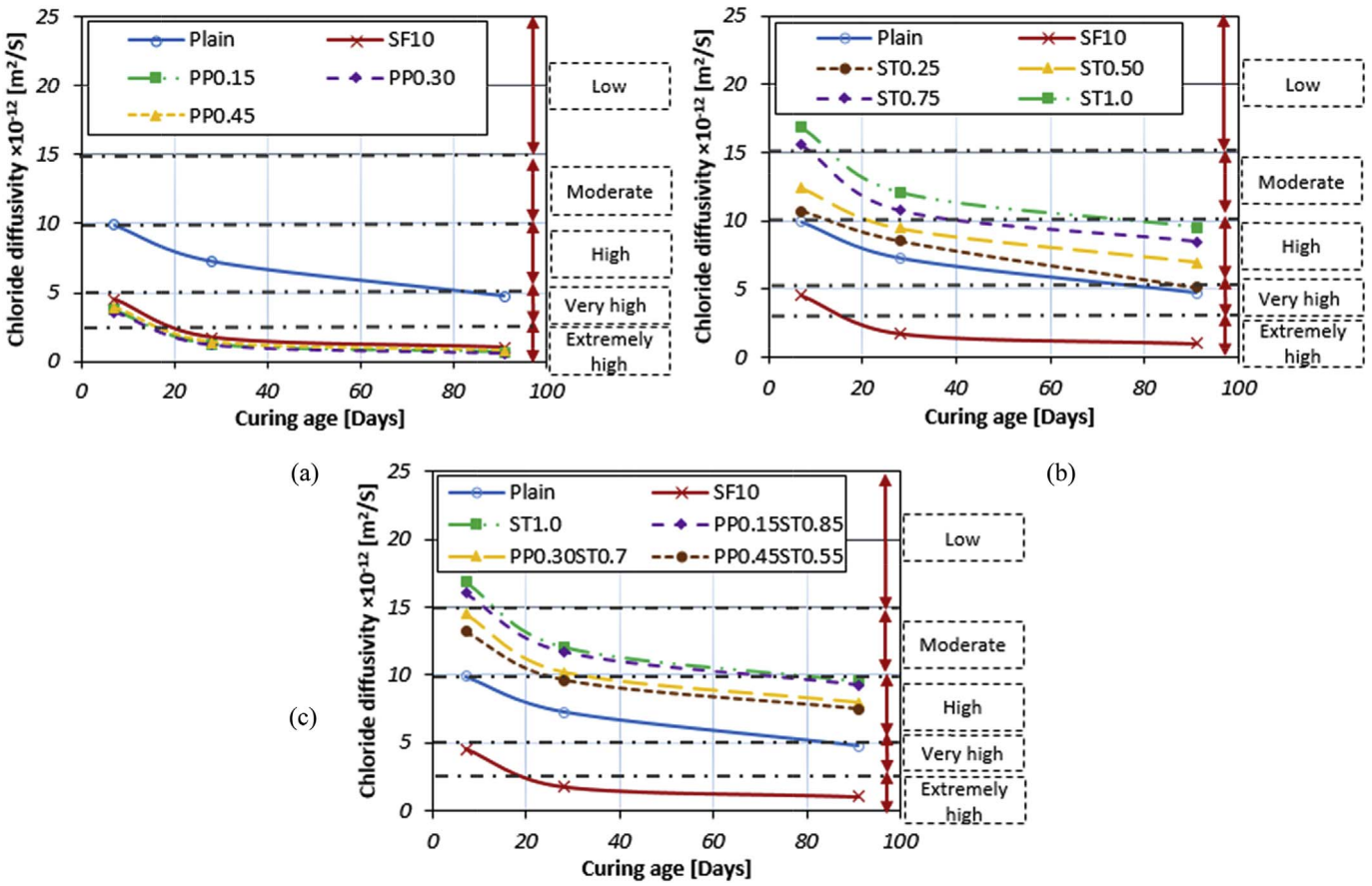

Fig. 6. Chloride diffusivity of different fiber-reinforced concretes: (a) polypropylene fiber-reinforced specimens, (b) steel fiber-reinforced specimens, and (c) hybrid fiber-reinforced specimen.

that replacement of OPC with 5% and 10% SF resulted in a reduction up to 46% and 73% on the permeability of concrete, respectively. Furthermore, Selvaraj et al. [69] and Dotto et al. [70] reported that introducing SF in concrete caused an important reduction on the corrosion rate of reinforced concrete. But, a slight increase in the corrosion rate of steel bars in concrete was indicated by Page and Havdahal [71]. As can be seen in Table 8, the efficiency of SF in the improvement of chloride diffusivity increased at a higher age. This is in close agreement with the results of other researchers, who found that the replacement of OPC with SF can lead to a decreased porosity of concrete, especially at a later age of curing [11,72,73]. According to the results obtained in this

Table 9
Resistance to chloride penetration of various types of concrete based on the 28-day chloride diffusivity [68].

Chloride diffusivity, $D_{28} \times 10^{-12}$ m^2/s	Classification of resistance to chloride penetration
> 15	Low
10–15	Moderate
5–10	High
2.5–5	Very high
< 2.5	Extremely high

Table 8
Results of chloride diffusivity and classification of corrosion rate.

Mix No.	Mixture ID	Chloride migration coefficient, $D \times 10^{-12}$ m^2/s			Classification of resistance to chloride penetration based on the chloride diffusivity		
		7 Days	28 Days	91 Days	7 Days	28 Days	91 Days
1	Plain	9.89	7.25	4.72	High	High	Very high
2	SF10	4.53	1.75	1.02	Very high	Extremely high	Extremely high
3	PP0.15	3.74	1.27	0.69	Very high	Extremely high	Extremely high
4	PP0.30	3.61	1.22	0.60	Very high	Extremely high	Extremely high
5	PP0.45	3.92	1.41	0.78	Very high	Extremely high	Extremely high
6	ST0.25	10.68	8.49	5.13	Moderate	High	High
7	ST0.50	12.39	9.42	6.95	Moderate	High	High
8	ST0.75	15.53	10.72	8.46	Low	Moderate	High
9	ST1.0	16.84	12.06	9.51	Low	Moderate	High
10	PP0.15ST0.85	16.04	11.69	9.22	Low	Moderate	High
11	PP0.30ST0.70	14.47	10.18	7.93	Moderate	Moderate	High
12	PP0.45ST0.55	13.20	9.61	7.45	Moderate	High	High

study and the classification of Table 9, the reference concrete and mix with 10% SF gained a “high” and “extremely high” resistance to chloride penetration for the 28-day specimen, respectively.

The results shown in Table 8 indicate that the combined use of SF and PP fibers in concrete led to a decrease in the chloride migration coefficient ranging from 60% to 87%, depending on the fiber content and testing age. This decrease can be attributed to the lower capillary porosity and reduced inner conductivity of pores, which in turn protect the steel bars in concrete from corrosion. As shown in Fig. 6, the chloride diffusivity was slightly increased by introducing 0.45% PP fiber, which can be related to the increased porosity of the mix. Toutanji [74] showed that the addition of SF in concretes made with PP fibers effectively reduced the chloride penetration as a result of improved fiber dispersion. The results of Ramezanianpour et al. [31] also confirmed that concrete samples reinforced with PP fibers had higher chloride penetration resistance due to a reduction in the inner conductivity of pores in which resulted in a lower probability of steel rebar corrosion. Based on the criteria listed in Table 9, polypropylene fiber-reinforced concretes were classified as having “very high” resistance to chloride penetration at 7 days, and “extremely high” resistance at 28 and 91 days. Because this experiment is related to a current that is passing from the surface of the concrete, the presence of conductive elements, such as steel fibers, significantly increased the chloride diffusivity of concrete. The results show that higher fiber volume fraction resulted in an increase in the chloride migration coefficient. It was observed that the chloride diffusivity of steel fiber-reinforced concretes was up to 101% greater than that of the reference specimen through the addition of 1.0% steel fiber. Meanwhile, some corroded materials occurred in the cathode solution of the steel fiber-reinforced concretes. Frazão et al. [40] also studied the durability of steel fiber-reinforced concretes by using rapid migration test and found that a slight increase in the chloride diffusivity of this mix occurred compared to that of the plain concrete. The growth of chloride ions in the fiber-paste interface weakened the protective oxide film of the steel fibers and subsequently increased the vulnerability of corrosion. It was also noted that the addition of SF in steel fiber-reinforced concretes mitigates the negative effect of steel fibers regarding the chloride migration resistance of concrete. As shown in Table 8, all the steel fiber-reinforced concretes were classified as having “high” resistance to chloride penetration after 91 days. The results indicated that substitution of a fraction of steel with PP fibers led to a decrease in the chloride diffusivity of concrete compared to that of the mix containing 1.0% steel fiber. The classification of HyFRCs varied from “low” to “high” resistance, depending on the fiber combination and testing age. As already noted, the crack width has a remarkable influence on the permeability resistance of concrete. Hoseini et al. [75] and Blunt et al. [43] showed that HyFRCs significantly reduce the corrosion rate of rebar, particularly when the concrete is subjected to load. This can be attributed to the appearance of multitude micro-cracks instead of the formation of a few large cracks.

3.7. Free drying shrinkage

The results of the free drying shrinkage tests for the FRCs are shown in Fig. 7. Furthermore, the results of drying shrinkage strain after 56 and 448 days for different specimens are depicted in Fig. 8. The replacement of OPC with 10% SF led to a reduction in the drying shrinkage strain of concrete of up to 9% over that of the plain concrete. This result shows that SF can reduce the porosity of concrete and produce a denser concrete with an increase in the C-S-H gel, which is a product of cement hydration with pozzolans. The findings of other researchers have also shown the efficiency of SF in the strengthening of a concrete structure by filling the small pores and increasing the density of hardened cement paste, which consequently reduces the drying shrinkage of concrete [76,77]. It has been shown that there was no significant distinction between the free shrinkage of different specimens in the initial days, while after 28 days, they showed a remarkable difference. Furthermore, the results show that the shrinkage occurred at a fast rate for early ages, and then the rate tended to stabilize after 224 days.

The results of FRCs demonstrate that the incorporation of fibers of any type and fiber content resulted in a reduction in the drying shrinkage of concrete. As shown in Fig. 7, a higher reduction in the shrinkage strain was attained as a result of increasing the fiber volume fraction. However, fiber content had more significant influence on the results of steel fiber-reinforced concretes. It was observed that a reduction in the drying shrinkage ranging from 11% to 18% and 13% to 21% was gained for PP and steel fiber-reinforced concretes, respectively, compared to that of the reference concrete. These results are in good agreement with the finding of other researchers, who found that introducing fibers in a composite can arrest cracking produced as a result of drying shrinkage [30,33,34]. For instance, Bywalski et al. [30] showed that the addition of 3% steel fibers led to a reduction up to 32% in the drying shrinkage of concrete. Barr et al. [78] studied the drying shrinkage of FRC at different water-cement ratios. It was reported that fibers had a negligible effect on the drying shrinkage of low strength concrete, whereas it caused a reduction on the drying shrinkage of HSC. In another study, Kim and Weiss [36] investigate the effect of different contents of steel fibers on the drying shrinkage of concrete. They indicated that the shrinkage strain was quite similar in all mixes irrespective to the fiber volume fraction. The results of HyFRCs indicate that the combined use of PP and steel fibers is a promising way to control the drying shrinkage of concrete. As cracks are initiated with small size and later propagated with different sizes in a body of concrete, hybridization of fibers with various features, such as different lengths and modulus of elasticity, plays an important role in resisting cracking at different scales and causes lower shrinkage. Among different concretes considered in this study, the best performing mix was attained by the mix containing 0.3% PP and 0.7% steel fibers; its shrinkage deformation was reduced up to 26% over that of the plain concrete. Furthermore, the results of FRCs show that the stabilization of the drying shrinkage occurred after 112 days.

4. Conclusions

This paper studies the effect of silica fume and fibers on the mechanical, chloride diffusivity and drying shrinkage of high-strength concrete. The following conclusions can be drawn from the experimental results:

1 Introducing silica fume and fibers in concrete results in a reduction in the workability of fresh concrete. Higher dosages of superplasticizers are required to maintain the same slump value as that of the plain concrete.
2 Silica fume in concrete mixtures leads to improvement in all properties of concrete, particularly the chloride diffusivity. Replacement of 10% of cement weight with silica fume in concrete led to a reduction of up to 78% in the chloride diffusivity of concrete.
3 The presence of fibers has a considerable influence on the mechanical properties of concrete. Steel fibers, due to their higher strength and modulus of elasticity, produced higher compressive strength and modulus of elasticity. An increase in the fiber volume fraction causes an increase in strength. Hybridization of fibers had no significant effect on the mechanical properties of concrete compared to those of the mix containing 1.0% steel fiber.
4 Inclusion of different types of fibers in concrete leads to dissimilar behavior in the longitudinal resonant frequency of concrete. The addition of PP fibers results in a reduction in the resonant frequency of concrete as a result of increased porosity. Meanwhile, the incorporation of steel fibers improves the resonant frequency of concrete. Likewise, the dynamic modulus of the elasticity test results shows a similar trend to those obtained for the resonant frequency tests.

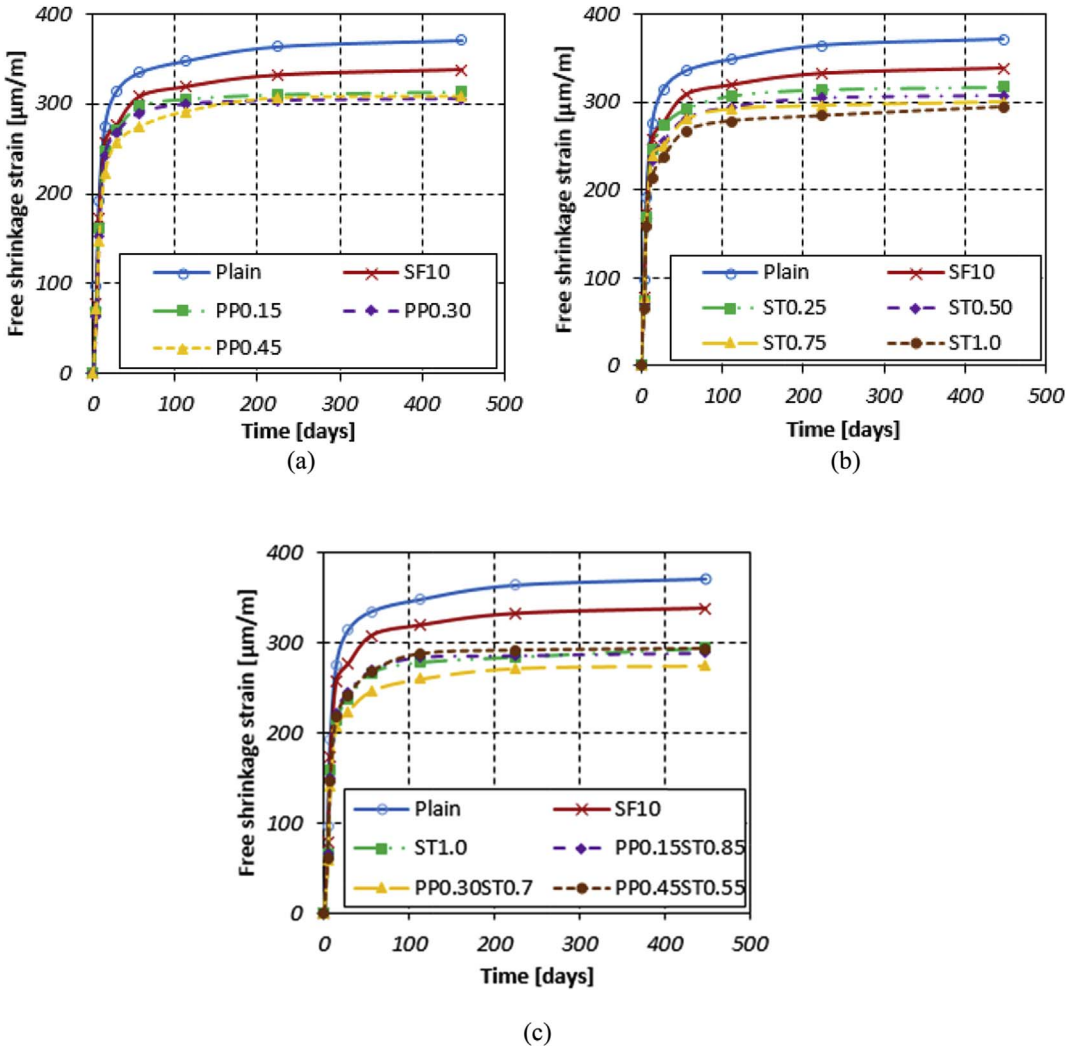

Fig. 7. Free drying shrinkage of different fiber-reinforced concretes: (a) polypropylene fiber-reinforced specimens, (b) steel fiber-reinforced specimens, and (c) hybrid fiber-reinforced specimens.

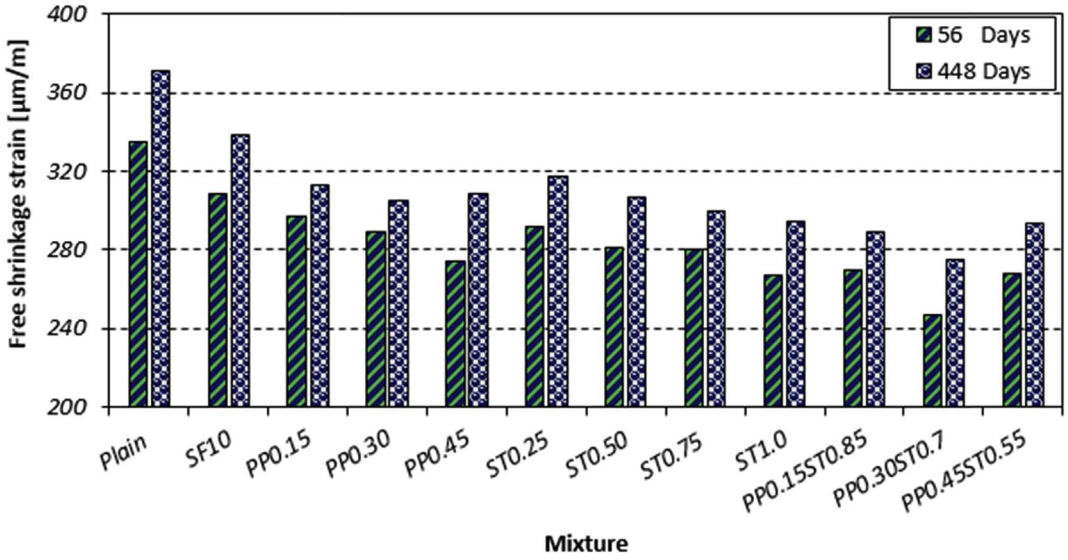

Fig. 8. Free drying shrinkage of different fiber-reinforced concretes at the time of 56 and 448 days.

5 The results indicate that the addition of PP fibers leads to a reduction in the chloride diffusivity of concrete due to the reduced inner conductivity of pores and lower capillary porosity. Meanwhile, the inclusion of steel fibers considerably increases the chloride diffusivity of concrete. This can be attributed to the conductivity of steel fibers, which increases the danger of corrosion in steel fiber-reinforced concretes.

6 The inclusion of fibers significantly reduces the drying shrinkage of concrete. However, it is found that increasing the fiber content has no significant influence on the results, particularly in the case of PP fibers. The lowest drying shrinkage was attained by the mix containing 0.3% PP and 0.7% steel fibers; its shrinkage strain was reduced up to 26% compared to that of the plain concrete.

The findings of this research are very promising and have the potential to significantly contribute toward expanding the use of HSC fabricated with PP and steel fibers to different structural applications. However, further research, particularly by using new type of steel fibers like double hooked-end steel fibers are needed to explore its effect on the bending behavior and time-dependent features (shrinkage and creep) of FRC, and the possibility of partial substitution of steel rebar reinforcement with fibers in structural applications.

References

[1] Celik K, Meral C, Mancio M, Mehta PK, Monteiro PJM. A comparative study of self-consolidating concretes incorporating high-volume natural pozzolan or high-volume fly ash. Constr Build Mater 2014;67:14–9.

[2] Biolzi L, Guerrini GL, Rosati G. Overall structural behavior of high strength concrete specimens. Constr Build Mater 1997;11(1):57–63.

[3] Afroughsabet V, Biolzi L, Ozbakkaloglu T. Influence of double hooked-end steel fibers and slag on mechanical and durability properties of high performance recycled aggregate concrete. Compos Struct 2017;181:273–84.

[4] Wang L, Zhou SH, Shi Y, Tang SW, Chen E. Effect of silica fume and PVA fiber on the abrasion resistance and volume stability of concrete. Compos Part B Eng 2017;130:28–37.

[5] Biolzi L, Cattaneo S, Guerrini GL. Fracture of plain and fiber-reinforced high strength mortar slabs with EA and ESPI monitoring. Appl Compos Mater 2000;7(1):1–12.

[6] Hung CC, Su YF, Su YM. Mechanical properties and self-healing evaluation of strain-hardening cementitious composites with high volumes of hybrid pozzolan materials. Compos Part B Eng 2018;133:15–25.

[7] Meng T, Yu Y, Wang Z. Effect of nano-CaCO 3 slurry on the mechanical properties and micro-structure of concrete with and without fly ash. Compos Part B Eng 2017;117:124–9.

[8] Gao Y, De Schutter G, Ye G, Tan Z, Wu K. The ITZ microstructure, thickness and porosity in blended cementitious composite: effects of curing age, water to binder ratio and aggregate content. Compos Part B Eng 2014;60:1–13.

[9] Rashiddadash P, Ramezanianpour AA, Mahdikhani M. Experimental investigation on flexural toughness of hybrid fiber reinforced concrete (HFRC) containing metakaolin and pumice. Constr Build Mater 2014;51:313–20.

[10] Johari MM, Brooks JJ, Kabir S, Rivard P. Influence of supplementary cementitious materials on engineering properties of high strength concrete. Constr Build Mater 2011;25(5):2639–48.

[11] Toutanji H, Delatte N, Aggoun S, Duval R, Danson A. Effect of supplementary cementitious materials on the compressive strength and durability of short-term cured concrete. Cem Concr Res 2004;34(2):311–9.

[12] Savino V, Lanzoni L, Tarantino AM, Viviani M. Simple and effective models to predict the compressive and tensile strength of HPFRC as the steel fiber content and type changes. Compos Part B Eng 2018;137:153–62.

[13] Nam J, Kim G, Lee B, Hasegawa R, Hama Y. Frost resistance of polyvinyl alcohol fiber and polypropylene fiber reinforced cementitious composites under freeze thaw cycling. Compos Part B Eng 2016;90:241–50.

[14] Afroughsabet V, Ozbakkaloglu T. Mechanical and durability properties of high-strength concrete containing steel and polypropylene fibers. Constr Build Mater 2015;94:73–82.

[15] Kim SW, Park WS, Jang YI, Feo L, Yun HD. Crack damage mitigation and shear behavior of shear-dominant reinforced concrete beams repaired with strain-hardening cement-based composite. Compos Part B Eng 2015;79:6–19.

[16] Şanal İ, Özyurt N, Hosseini A. Characterization of hardened state behavior of self compacting fiber-reinforced cementitious composites (SC-FRCC's) with different beam sizes and fiber types. Compos Part B Eng 2016;105:30–45.

[17] Gesoglu M, Güneyisi E, Muhyaddin GF, Asaad DS. Strain hardening ultra-high performance fiber reinforced cementitious composites: effect of fiber type and concentration. Compos Part B Eng 2016;103:74–83.

[18] Afroughsabet V, Biolzi L, Ozbakkaloglu T. High-performance fiber-reinforced concrete: a review. J Mater Sci 2016;51(14):6517–51.

[19] Simões T, Octávio C, Valença J, Costa H, Dias-da-Costa D, Júlio E. Influence of concrete strength and steel fibre geometry on the fibre/matrix interface. Compos Part B Eng 2017;122:156–64.

[20] Nili M, Afroughsabet V. Combined effect of silica fume and steel fibers on the impact resistance and mechanical properties of concrete. Int J impact Eng 2010;37(8):879–86.

[21] Meng W, Khayat KH. Improving flexural performance of ultra-high-performance concrete by rheology control of suspending mortar. Compos Part B Eng 2017;117:26–34.

[22] Choi WC, Yun HD, Cho CG, Feo L. Attempts to apply high performance fiber-reinforced cement composite (HPFRCC) to infrastructures in South Korea. Compos Struct 2014;109:211–23.

[23] Banthia N, Gupta R. Hybrid fiber reinforced concrete (HyFRC): fiber synergy in high strength matrices. Mater Struct 2004;37(10):707–16.

[24] Choi WC, Jang SJ, Yun HD. Bond and cracking behavior of lap-spliced reinforcing bars embedded in hybrid fiber reinforced strain-hardening cementitious composite (SHCC). Compos Part B Eng 2017;108:35–44.

[25] Jen G, Trono W, Ostertag CP. Self-consolidating hybrid fiber reinforced concrete: development, properties and composite behavior. Constr Build Mater 2016;104:63–71.

[26] Corinaldesi V, Nardinocchi A. Mechanical characterization of Engineered Cement-based Composites prepared with hybrid fibres and expansive agent. Compos Part B Eng 2016;98:389–96.

[27] Caggiano A, Folino P, Lima C, Martinelli E, Pepe M. On the mechanical response of hybrid fiber reinforced concrete with recycled and industrial steel fibers. Constr Build Mater 2017;147:286–95.

[28] Qian C, Stroeven P. Fracture properties of concrete reinforced with steel–polypropylene hybrid fibres. Cem Concr Compos 2000;22(5):343–51.

[29] Caggiano A, Gambarelli S, Martinelli E, Nisticò N, Pepe M. Experimental characterization of the post-cracking response in hybrid steel/polypropylene fiber-reinforced concrete. Constr Build Mater 2016;125:1035–43.

[30] Bywalski C, Kamiński M, Maszczak M. Influence of steel fibres addition on mechanical and selected rheological properties of steel fibre high-strength reinforced concrete. Archives Civ Mech Eng 2015;15(3):742–50.

[31] Ramezanianpour AA, Esmaeili M, Ghahari SA, Najafi MH. Laboratory study on the effect of polypropylene fiber on durability, and physical and mechanical characteristic of concrete for application in sleepers. Constr Build Mater 2013;44:411–8.

[32] Toutanji H, McNeil S, Bayasi Z. Chloride permeability and impact resistance of polypropylene-fiber-reinforced silica fume concrete. Cem Concr Res 1998;28(7):961–8.

[33] Kaïkea A, Achoura D, Duplan F, Rizzuti L. Effect of mineral admixtures and steel fiber volume contents on the behavior of high performance fiber reinforced concrete. Mater Des 2014;63:493–9.

[34] Choi SY, Park JS, Jung WT. A study on the shrinkage control of fiber reinforced concrete pavement. Procedia Eng 2011;14:2815–22.

[35] Sun W, Chen H, Luo X, Qian H. The effect of hybrid fibers and expansive agent on the shrinkage and permeability of high-performance concrete. Cem Concr Res 2001;31(4):595–601.

[36] Kim B, Weiss WJ. Using acoustic emission to quantify damage in restrained fiber-reinforced cement mortars. Cem Concr Res 2003;33(2):207–14.

[37] Sargaphuti M, Shah SP, Vinson KD. Shrinkage cracking and durability characteristics of cellulose fiber reinforced concrete. ACI Mater J 1993;90(4):309–18.

[38] Grzybowski M, Shah SP. Shrinkage cracking of fiber reinforced concrete. ACI Mater J 1990;87(2):138–48.

[39] Behfarnia K, Behravan A. Application of high performance polypropylene fibers in concrete lining of water tunnels. Mater Des 2014;55:274–9.

[40] Frazão C, Camões A, Barros J, Gonçalves D. Durability of steel fiber reinforced self-compacting concrete. Constr Build Mater 2015;80:155–66.

[41] ACI Committee 318. Building code requirements for reinforced concrete ACI 318–08 Detroit, Michigan: American Concrete Institute; 2008.

[42] ACI Committee 224R. Control of cracking in concrete structures ACI 224–01 Detroit, Michigan: American Concrete Institute; 2001.

[43] Blunt J, Jen G, Ostertag CP. Enhancing corrosion resistance of reinforced concrete structures with hybrid fiber reinforced concrete. Corros Sci 2015;92:182–91.

[44] ASTM C 143. Standard test method for slump of hydraulic-cement concrete. 2010.

[45] ASTM C 39. Standard test method for compressive strength of cylindrical concrete specimens. 2003.

[46] ASTM C 469. Standard test method for static modulus of elasticity and Poisson's ratio of concrete in compression. 2014.

[47] BS 1881-209. Testing concrete. Recommendations for the measurement of dynamic modulus of elasticity. 1990.

[48] Mosley WH, Hulse R, Bungey JH. Reinforced concrete design: to eurocode 2. Palgrave macmillan; 2012.

[49] ASTM C 157. Standard test method for length change of hardened hydraulic-cement mortar and concrete. 1993.

[50] NT BUILD 492. Concrete, mortar and cement-based repair materials: chloride migration coefficient from non-steady-state migration experiments. Nordtest Method. 1999.

[51] Nili M, Afroughsabet V. Property assessment of steel–fibre reinforced concrete made with silica fume. Constr Build Mater 2012;28(1):664–9.

[52] Kim JE, Park WS, Jang YI, Kim SW, Kim SW, Nam YH, Kim DG, Rokugo K. Mechanical properties of energy efficient concretes made with binary, ternary, and quaternary cementitious blends of fly ash, blast furnace slag, and silica fume. Int J Concr Struct Mater 2016;10(3):97–108.

[53] Wu K, Shi H, Xu L, Ye G, De Schutter G. Microstructural characterization of ITZ in blended cement concretes and its relation to transport properties. Cem Concr Res 2016;79:243–56.

[54] Yan H, Sun W, Chen H. The effect of silica fume and steel fiber on the dynamic mechanical performance of high-strength concrete. Cem Concr Res 1999;29(3):423–6.
[55] Khayat KH, Kassimi F, Ghoddousi P. Mixture design and testing of fiber-reinforced self-consolidating concrete. ACI Mater J 2014;111(2):143–51.
[56] Rahmani E, Dehestani M, Beygi MHA, Allahyari H, Nikbin IM. On the mechanical properties of concrete containing waste PET particles. Constr Build Mater 2013;47:1302–8.
[57] Khaloo AR, Esrafili A, Kalani M, Mobini MH. Use of polymer fibres recovered from waste car timing belts in high performance concrete. Constr Build Mater 2015;80:31–7.
[58] Hernandez-Olivares F, Barluenga G, Bollati M, Witoszek B. Static and dynamic behaviour of recycled tyre rubber-filled concrete. Cem Concr Res 2002;32(10):1587–96.
[59] Söylev TA, Özturan T. Durability, physical and mechanical properties of fiber-reinforced concretes at low-volume fraction. Constr Build Mater 2014;73:67–75.
[60] Mehta PK, Monteiro PJ. Concrete: microstructure, properties, and materials. McGraw-Hill; 2006.
[61] Bolat H, Şimşek O, Çullu M, Durmuş G, Can Ö. The effects of macro synthetic fiber reinforcement use on physical and mechanical properties of concrete. Compos Part B Eng 2014;61:191–8.
[62] Aslani F, Nejadi S. Self-compacting concrete incorporating steel and polypropylene fibers: compressive and tensile strengths, moduli of elasticity and rupture, compressive stress–strain curve, and energy dissipated under compression. Compos Part B Eng 2013;53:121–33.
[63] Hassan AMT, Jones SW. Non-destructive testing of ultra high performance fibre reinforced concrete (UHPFRC): a feasibility study for using ultrasonic and resonant frequency testing techniques. Constr Build Mater 2012;35:361–7.
[64] Shi X, Xie N, Fortune K, Gong J. Durability of steel reinforced concrete in chloride environments: an overview. Constr Build Mater 2012;30:125–38.
[65] Hannawi K, Bian H, Prince-Agbodjan W, Raghavan B. Effect of different types of fibers on the microstructure and the mechanical behavior of Ultra-High Performance Fiber-Reinforced Concretes. Compos Part B Eng 2016;86:214–20.
[66] Berrocal CG, Lundgren K, Löfgren I. Corrosion of steel bars embedded in fibre reinforced concrete under chloride attack: state of the art. Cem Concr Res 2016;80:69–85.
[67] Zhang MH, Li H. Pore structure and chloride permeability of concrete containing nano-particles for pavement. Constr Build Mater 2011;25(2):608–16.
[68] Nilsson L, Ngo MH, Gjørv OE. High-performance repair materials for concrete structures in the port of Gothenburg. Second international conference on concrete under severe conditions: environment and loading. vol. 2. 1998. p. 1193–8.
[69] Selvaraj R, Muralidharan S, Srinivasan S. The influence of silica fume on the factors affecting the corrosion of reinforcement in concrete-a review. Struct Concr 2003;4(1):19–23.
[70] Dotto JMR, De Abreu AG, Dal Molin DCC, Müller IL. Influence of silica fume addition on concretes physical properties and on corrosion behaviour of reinforcement bars. Cem Concr Compos 2004;26(1):31–9.
[71] Page CL, Havdahl J. Electrochemical monitoring of corrosion of steel in microsilica cement pastes. Mater Struct 1985;18(1):41–7.
[72] Elahi A, Basheer PAM, Nanukuttan SV, Khan QUZ. Mechanical and durability properties of high performance concretes containing supplementary cementitious materials. Constr Build Mater 2010;24(3):292–9.
[73] Kaid N, Cyr M, Julien S, Khelafi H. Durability of concrete containing a natural pozzolan as defined by a performance-based approach. Constr Build Mater 2009;23(12):3457–67.
[74] Toutanji HA. Properties of polypropylene fiber reinforced silica fume expansive-cement concrete. Constr Build Mater 1999;13(4):171–7.
[75] Hoseini M, Bindiganavile V, Banthia N. The effect of mechanical stress on permeability of concrete: a review. Cem Concr Compos 2009;31(4):213–20.
[76] Li J, Yao Y. A study on creep and drying shrinkage of high performance concrete. Cem Concr Res 2001;31(8):1203–6.
[77] Güneyisi E, Gesoğlu M, Özbay E. Strength and drying shrinkage properties of self-compacting concretes incorporating multi-system blended mineral admixtures. Constr Build Mater 2010;24(10):1878–87.
[78] Barr B, Hoseinian SB, Beygi MA. Shrinkage of concrete stored in natural environments. Cem Concr Compos 2003;25(1):19–29.